ATP-EMTP evaluation of relaying algorithms for series-compensated line

M. M. Saha, E. Rosolowski, J. Izykowski, P. Pierz

***Abstract*—A group of the algorithms aimed at measuring a fault-loop impedance for digital distance relay has been considered. The algorithms gathered in two basic families have been tested: – methods based upon Fourier orthogonal components with using both full-cycle and half-cycle data windows; – methods founded on differential equation techniques (four variants with applied various digital differentiation rules and additional pre-filtration). Extensive simulation studies have been performed for comparing the measuring techniques. Recommendations with respect to impedance algorithms for protection of series compensated lines are stated. The other studied algorithm is related with fault direction discrimination for the considered series compensated line arrangement. Sample simulation results are presented and discussed.**

***Keywords*: transmission line, series capacitor compensation, faults, digital distance protection, impedance algorithms, ATP-EMTP simulation.**

I. Introduction

Increased transmittable power, improved power system stability, reduced transmission losses, improved voltage control and flexible power flow control are the primarily reasons behind installing Series Capacitors (SCs) on long power transmission lines. The installation costs usually do not exceed 15-30% of a new line and are not affected by the environmental concerns [1]. SCs, when set on a line, create, however, certain problems for its protective devices [2], [3] and fault locators [4].

When a series compensated line suffers a fault behind its SCs, as seen from the relaying point (Fig. 1 – fault F_2 for the Relay A and the fault F_1 for the Relay B), a fault loop considered by a distance relay contains, depending on type of fault, one or even two complexes of SCs and their overvoltage protecting arresters (usually Metal-Oxide Varistors (MOVs)). The presence of MOVs makes a fault loop strongly nonlinear and nature of transients of the relaying signals is entirely different than for traditional lines [1].

Improvement of series compensated line protection calls for detailed investigation of both impedance measuring algorithms and auxiliary algorithms dedicated for fault detection, phase selection, direction detection. This paper is focused on speeding-up the measurement of a fault-loop impedance. In case of the considered protection, a high speed is expected, while for fault location for an inspection-repair purpose a speed is not important and thus complex calculations can be applied, as for example as presented in [5]–[7].

The other contribution of this paper relies on investigation of the algorithm for fault direction discrimination [8], also in an environment of the studied arrangement (Fig.1).

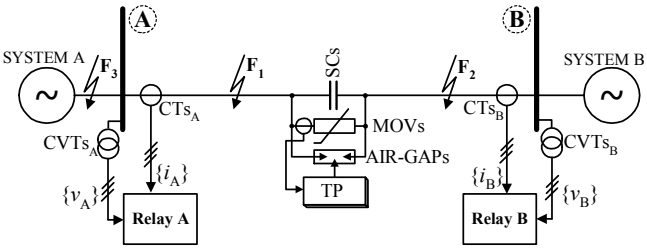

Fig. 1. Schematic diagram of the studied series compensated system

The software package ATP-EMTP [9] was used for generating fault data under versatile faults on the line. A single-circuit fully transposed transmission line A–B (Fig. 1) is considered as compensated at 70% rate with a three-phase bank of series capacitors (SCs) installed in the middle.

Calculation of the fault loop impedance used for comparing with an impedance characteristic requires selecting proper relaying voltage and current. This is a state of the art of distance protection technique [1], [10]. In case of the considered here fully transposed line, the residual-current compensation is applied for phase-to-earth faults. In turn, for unsymmetrical lines [10] the phase-current-compensation technique has to be applied.

II. Model of Series Compensated Line

The line (300 km, 400 kV, 50 Hz) is modeled using the transposed Clarke model. Line impedances for the positive- and zero-sequence were assumed in modeling as:
Z_{1L}=0.315 Ω/km, 85°; Z_{0L}=1.0265 Ω/km, 75°.

The MOVs were modeled as non-linear resistors approximated by the standard *v*–*i* characteristic (Fig. 2c):

$$i = P\left(\frac{v}{V_{\mathrm{REF}}}\right)^{q} \tag{1}$$

where: q, P, V_{REF} MOV parameters. The parameters of (1) assumed in this study were: q=23, P=1 kA, V_{REF}=150 kV.

Each MOV is protected from overheating by firing the complementary air-gap by the thermal (overload) protection

M. M. Saha is with ABB AB, S-721 59, Västerås, Sweden (e-mail of corresponding author: murari.saha@se.abb.com).
E. Rosolowski, J. Izykowski and P. Pierz are with Wroclaw University of Technology, Wybrzeze Wyspianskiego 27, 50-370 Wroclaw, Poland (e-mails: {eugeniusz.rosolowski; jan.izykowski; piotr.pierz}@pwr.edu.pl).

Paper submitted to the International Conference on Power Systems Transients (IPST2015) in Cavtat, Croatia June 15-18, 2015

(Fig. 2). The MOV protection was modeled as energy-based using ATP-EMTP MODELS: the energy absorbed by the MOV is integrated and the MOV becomes shunted by firing the air-gap (the signal DOWN causes closing of the type 13 switch) when this energy reaches its pre-defined limit.

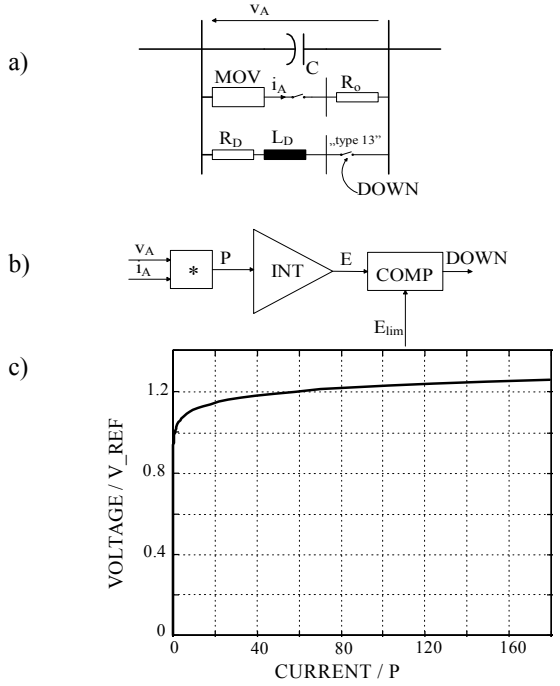

Fig. 2. Modelling of series capacitor equipped with MOV: a) adopted scheme, b) structure of algorithm for thermal protection of MOV, c) voltage-current characteristic of MOV.

The relay measuring chain was modeled as well. Capacitive Voltage Transformers (CVTs) were represented by their 4th order linear models while Current Transformers (CTs) were simulated taking into account their saturation branches. The analog anti-aliasing filters were represented by the 2nd order approximation with the cut-off frequency set at $1/3$ of the sampling rate f_s (f_s=1 kHz was assumed in this study).

Variety of conditions with respect to the supplying systems were considered. In all the tests of this paper the impedances of the local (A) and remote (B) sources were taken as identical and equal to: $Z_{s1}=Z_{s2}=15\ \Omega, 85^o$, $Z_{s0}=26.6\ \Omega, 85^o$. The remote sources were delayed by 10^o with respect to the local sources.

III. Fourier Methods

Distance protection of a transmission line requires measurement of a fault loop impedance (R, X). Comparison of the measured impedance with the characteristics properly shaped on an impedance plan enables to make a decision whether a fault occurred in the protection zone or not. In order to provide adequately fast disconnection of a faulted line such a decision ought to be made very fast – within time shorter than a fundamental frequency period for modern relays.

The aim of this study is to develop the measuring algorithm for fast operating relays applied for protection of series compensated lines. First, the Fourier methods have been taken into consideration. According to them impedance components (R, X) of a fault loop are estimated with the orthogonal components of voltage and current from a fault-loop [1]:

$$R = \frac{u_c i_c + u_s i_s}{i_c^2 + i_s^2}$$
$$X = \frac{u_s i_c - u_c i_s}{i_c^2 + i_s^2} \qquad (2)$$

where: u_c, i_c, u_s, i_s direct (cosine) and quadratic (sine) orthogonal components of voltage and current, respectively.

Both the full-cycle and the half-cycle Fourier algorithms for calculation of the orthogonal components are considered.

The sample a-b fault at 250 km from the substation A with fault resistance 0.1 Ω (Fig. 1 – fault F_2) is taken for showing performance of the considered algorithms.

Figs. 3A and 3B presents phase voltages and currents at both the substations. The relay at the substation A sees this fault as behind the SCs&MOVs, while the relay at the substation B – as on a conventional line (i.e. not compensated). High frequency distortion of the waveforms is more visible in the case of the substation A (caused by the MOVs switching between linear and non-linear operating modes). The phase currents at the substation B contain, analogously as in uncompensated lines, the DC components.

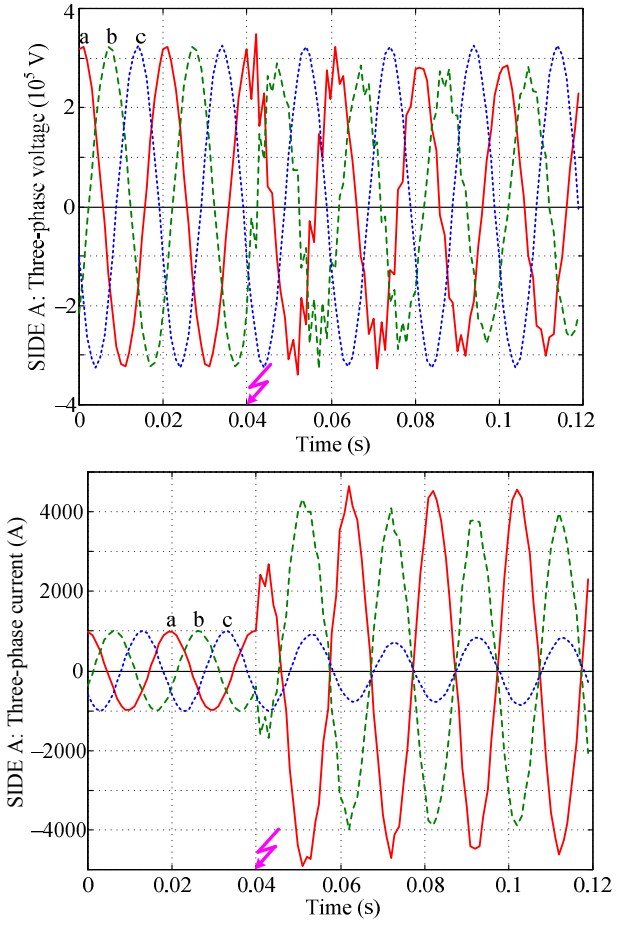

Fig. 3A. Three-phase voltage and current signals measured at the substation A under the sample a-b fault.

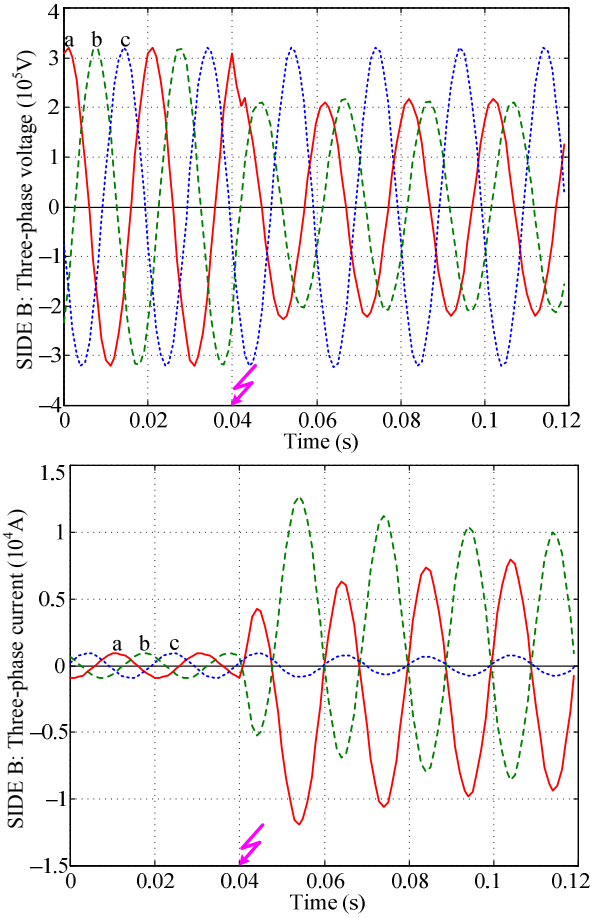

Fig. 3B. Three-phase voltage and current signals measured at the substation B under the sample a-b fault.

Fig. 4 depicts the estimation of impedance seen from the substations A and B using the full-cycle Fourier algorithm. The estimates measured at the substation A settle almost after 30 ms, what is not acceptable for modern ultra-high speed relays. On the other hand, the estimates at the substation B (the corresponding fault loop does not contain the SCs&MOVs) settle after 20 ms (the window length). The large overshoots result from the phase inversion of the side B currents.

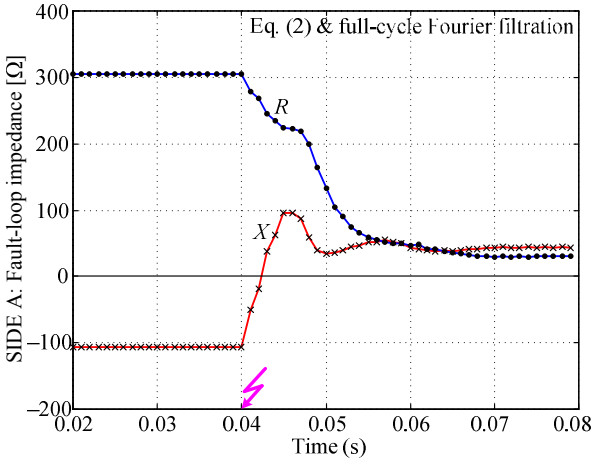

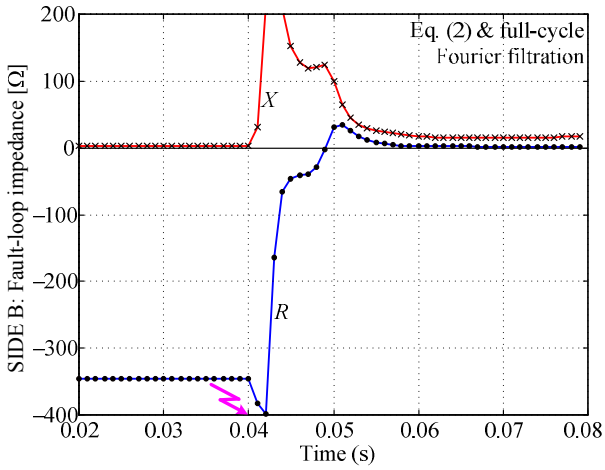

Fig.4. Fault loop impedance estimation with the use of Fourier full-cycle filters.

Fig. 5 displays the impedance estimation with the use of half-cycle Fourier filters. The impedance at the substation A settles after some 30 ms (also unacceptable) and one observes the danger of dynamic overreaching. The impedance at the substation B settles after 10 ms (the window length).

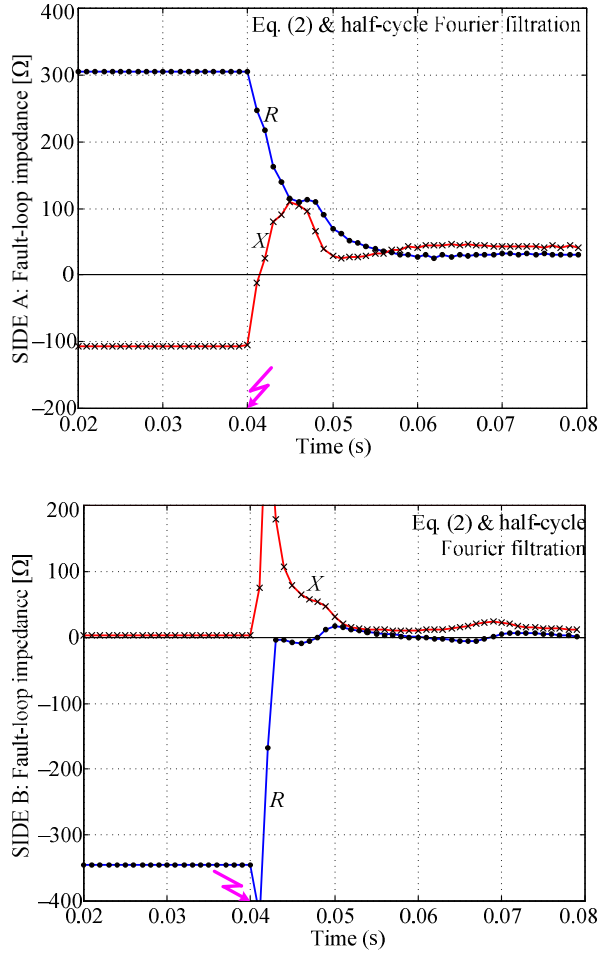

Fig. 5. Fault loop impedance estimation with the use of Fourier half-cycle filters.

The results of the tests from Figs. 4 and 5 clearly show that the Fourier methods are not suitable for series compensated line protection.

IV. Differential Equation Methods for Impedance Measurement

It is assumed that the fault loop circuit is described analogously as for a traditional (uncompensated) line by the following differential equation:

$$Ri(t) + L\frac{di(t)}{dt} = u(t) \tag{3}$$

It is worth to notice that in (3) u and i are measured, while R and L are to be estimated. To obtain a measuring algorithm the eq. (3) must be first written in a digital form:

$$\begin{aligned} Ra_1 + Ld_1 &= b_1 \\ Ra_2 + Ld_2 &= b_2 \end{aligned} \tag{4}$$

from which the sought values R and L are derived constituting the impedance algorithm:

$$\begin{aligned} R &= \frac{d_1 b_2 - d_2 b_1}{a_2 d_1 - a_1 d_2} \\ X &= \frac{a_2 b_1 - a_1 b_2}{a_2 d_1 - a_1 d_2}\omega_1 \end{aligned} \tag{5}$$

where: ω_1 – the radian fundamental frequency, a_1, a_2, b_1, b_2, d_1, d_2 – coefficients dependent on the way of digital approximation of (3).

A. Differential equation method with application of rectangular differentiation

The operator of differentiation in the continuous time in (3) is replaced by the rectangular numerical rule [1] in the discrete time domain. To obtain proper phase shift introduced by this operation (+90° for the fundamental frequency), averages for two successive samples of u and i are taken instead of samples of these signals directly. In order to originate two independent equations, (3) is written for two successive samples and the coefficients in (4) are:

$$\begin{aligned} a_1 &= \frac{1}{2}\left[i(k) + i(k-1)\right] & a_2 &= \frac{1}{2}\left[i(k-1) + i(k-2)\right] \\ b_1 &= \frac{1}{2}\left[u(k) + u(k-1)\right] & b_2 &= \frac{1}{2}\left[u(k-1) + u(k-2)\right] \\ d_1 &= \frac{1}{T}\left[i(k) - i(k-1)\right] & d_2 &= \frac{1}{T}\left[i(k-1) - i(k-2)\right] \end{aligned} \tag{6}$$

where: T – sampling period.

Fig. 6 presents the estimation process with the use of this method (the equation (5) combined with the formulas (6)) for the same fault case as before in Figs. 4 and 5. The measurement at the substation B (no SCs&MOVs in a fault loop) is very fast (below 5 ms) and accurate (no dynamic overreaching, no oscillations). However, when executed at the side A, for which a fault loop contains SCs&MOVs, poor time response of the algorithm is observed. Large oscillations caused by the MOVs switching between linear and non-linear operating modes are observed. Such oscillations are definitely unacceptable.

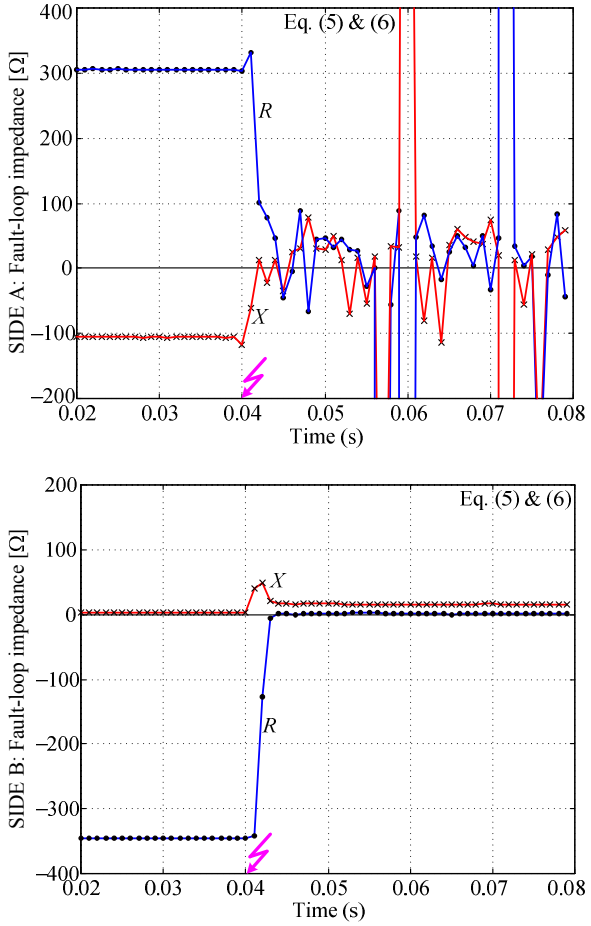

Fig. 6. Fault loop impedance estimation with the use of differential equation based method with rectangular differentiation

B. Differential equation method with application of rectangular differentiation and digital pre-filtration

The algorithm from the subsection A displays significant dynamic errors due to mismatch of the used model of the process (differential equation for the R–L circuit) and the actual process (first of all operation of SCs&MOVs; line shunt capacitances; transients of CTs, CVTs and analogue filters). This generates noise in the estimates, located mainly in the high frequency region. Therefore, measurement may be improved by applying additional pre-filtration of the voltage and current signals prior executing (6) and (5). Consequently, (6) is replaced by (7):

$$\begin{aligned} a_1 &= \frac{1}{2}\left[i_f(k) + i_f(k-1)\right] & a_2 &= \frac{1}{2}\left[i_f(k-1) + i_f(k-2)\right] \\ b_1 &= \frac{1}{2}\left[u_f(k) + u_f(k-1)\right] & b_2 &= \frac{1}{2}\left[u_f(k-1) + u_f(k-2)\right] \\ d_1 &= \frac{1}{T}\left[i_f(k) - i_f(k-1)\right] & d_2 &= \frac{1}{T}\left[i_f(k-1) - i_f(k-2)\right] \end{aligned} \tag{7}$$

where: subscript f denotes digital pre-filtration.

The pre-filtration has been done using Fourier half-cycle cosine filter for both current and voltage signals. Such the pre-filtration of low-pass type is reasonable for this particular application as the DC components are eliminated by the equation (5) itself.

Fig. 7 presents the measurement process using the method (5) combined with (7) for the same fault case as before in Figs. 4, 5, 6. The impedance seen from the substation B settles in some 10 ms (length of the data window for the pre-filtration). In turn, as seen from the substation A (SCs&MOVs in a fault loop), the settling time for the resistance and the reactance is around a half fundamental frequency cycle. As a result of pre-filtration the high frequency oscillations are removed from the resulting impedance components (compare with Fig. 6).

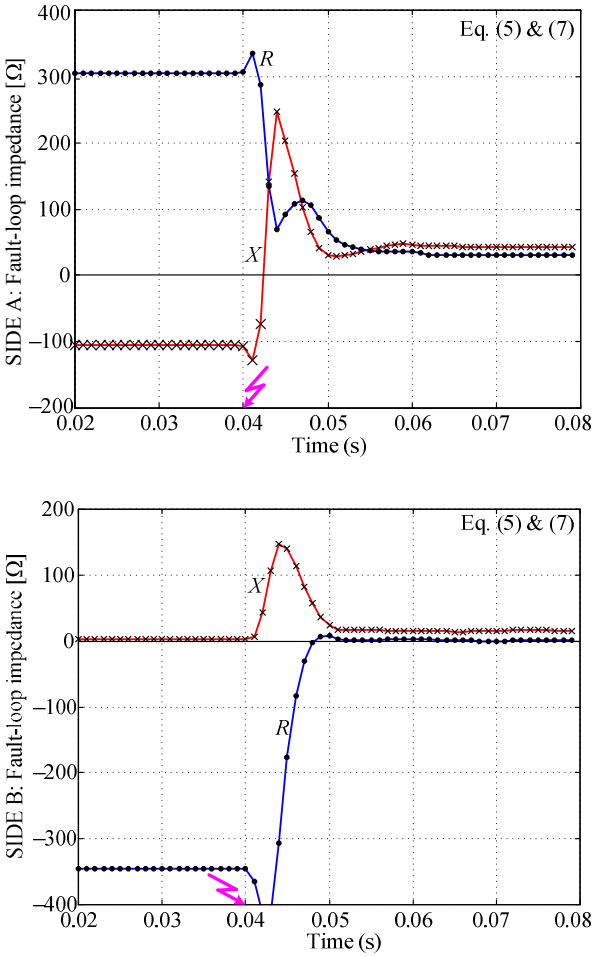

Fig. 7. Fault loop impedance estimation with the use of differential equation based method with rectangular differentiation and half-cycle pre-filtration.

C. Differential equation method with application of Gear differentiation rule

This method is a variant of the method defined in the subsection B. The rectangular rule is replaced by the three-point Gear differentiation [11] which introduces for the fundamental frequency exactly 90° phase shift between the signal and its numerically computed derivative. Consequently, no additional (compensating) computations are needed for the signals (as it was necessary in the method described in the subsection B). It is, however, necessary to apply an extra pre-filtration too. Thus, the equations replacing (7) are as follows:

$$
\begin{aligned}
&a_1 = i_f(k),\ a_2 = i_f(k-1),\\
&b_1 = u_f(k),\ b_2 = u_f(k-1),\\
&d_1 = \frac{\omega_1}{d}\left[3i_f(k) - 4i_f(k-1) + i_f(k-2)\right],\\
&d_2 = \frac{\omega_1}{d}\left[3i_f(k-1) - 4i_f(k-2) + i_f(k-3)\right],
\end{aligned}
\qquad (8)
$$

where:

$$
d = 2\sqrt{(1-\cos(\frac{2\pi}{N}))^2 + \left(2\sin(\frac{2\pi}{N}) - \frac{1}{2}\sin(\frac{4\pi}{N})\right)^2},
$$

N – number of samples in one fundamental freq. cycle.

As in subsection B, half-cycle cosine Fourier filters have been used for the digital pre-filtration of both voltage and current signals (the subscript f). Fig. 8 presents the example of the measuring process with the use of this method for the same fault case as before in Figs. 4, 5, 6, 7. At the substation A the settling time is around three quarters of a cycle, while about half a cycle for the substation B. The algorithm performs similarly as the algorithm from the subsection B.

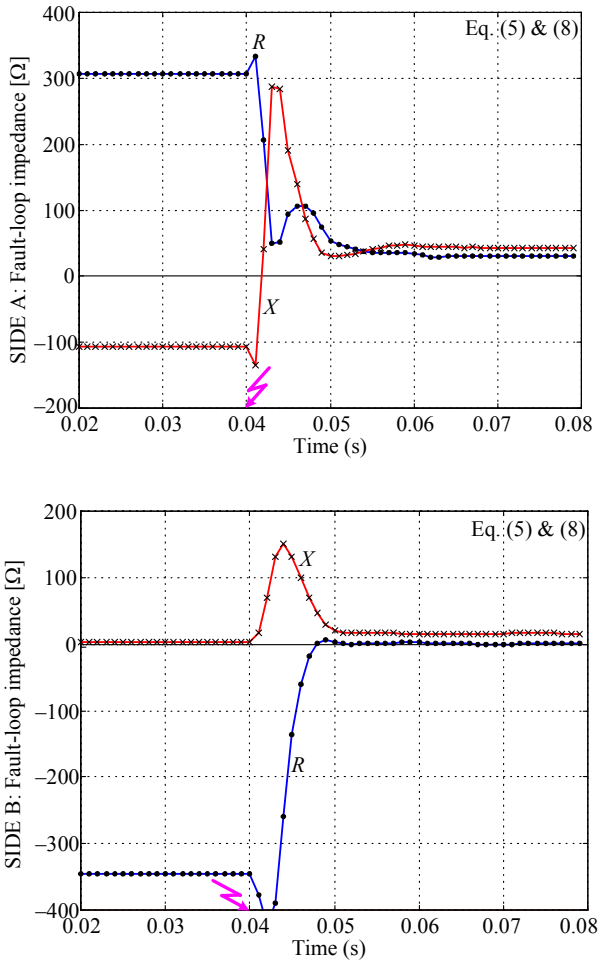

Fig. 8. Fault loop impedance estimation with the use of differential equation based method with Gear three point differentiation and half-cycle pre-filtration

D. Differential equation method with application of rectangular differentiation and orthogonal components

In this method, the current and voltage signals are first split into their orthogonal components as the differential equation (3) is valid for both direct and quadratic components of the signals. Solving such as system with respect to sought R and X one gets the measuring algorithm in the form of (5), but combined with the following coefficients:

$$a_1 = \frac{1}{2}\left[i_s(k) + i_s(k-1)\right] \qquad a_2 = \frac{1}{2}\left[i_c(k-1) + i_c(k-2)\right]$$
$$b_1 = \frac{1}{2}\left[u_s(k) + u_s(k-1)\right] \qquad b_2 = \frac{1}{2}\left[u_c(k-1) + u_c(k-2)\right] \quad (9)$$
$$d_1 = \frac{1}{T}\left[i_s(k) - i_s(k-1)\right] \qquad d_2 = \frac{1}{T}\left[i_c(k-1) - i_c(k-2)\right]$$

where: subscripts s, c denote quadratic (sine) and direct (cosine) orthogonal components.

In this paper Fourier half-cycle sine/cosine filters have been used to extract the orthogonal components of both current and voltage. Fig. 9 displays the sample results of applying the algorithm (5) in combination with (9) for the previously used test fault. They illustrate good performance of this algorithm, as at both ends of the line the settling time is shorter than a cycle.

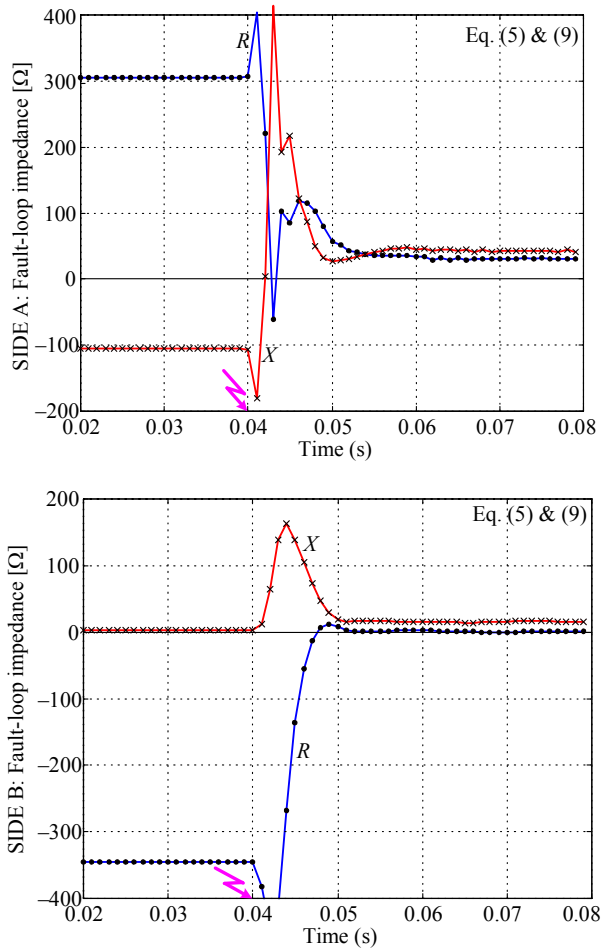

Fig. 9. Fault loop impedance estimation with the use of differential equation based method with rectangular differentiation combined with orthogonal components.

V. Fault Direction Discrimination

The phenomena specific to a series compensated line affect also the auxiliary functions of its distance relay including fault detection, phase selection and direction detection. All these blocks are essentially important for the overall performance of the complete distance relay.

A directional element becomes essential for a complete distance relay when a fault to be cleared occurs very close to a relaying point. The traditional approach to mitigate the problem of the voltage fall is to apply an additional polarization voltage. It may be done by [1]:

(a) cross polarization of a voltage signal,

(b) memory polarization of a voltage signal.

Also, a combination of the above two approaches is possible. Further improvement is achieved when processing the change in current signals. This idea applies full cross polarization for the directional measurement. The polarizing voltage is taken entirely from the healthy phases. The change in the phase current is used for the directionality to eliminate the influence of load current. An impedance is calculated for each phase. As for example, for the phase a, the impedance is calculated by utilizing:

$$\underline{Z}_{\mathrm{a}} = \frac{\underline{U}_{\mathrm{bc}}}{\underline{I}_{\mathrm{a\_flt}} - \underline{I}_{\mathrm{a\_pre}}} \quad (10)$$

For the detection of fault in „forward direction" the argument for the calculated „impedance" shall be within: –15 to 115 degrees [1].

McLaren et al. [8] rearranged the well-known direction detection principle for fast acting numerical relays. The concept is based on computing the incremental positive sequence impedance defined by the increments (pre-fault quantities subtracted from the fault ones) in positive sequence of voltage and current:

$$\Delta\underline{Z}_1 = \frac{(\underline{U}_{\mathrm{flt}} - \underline{U}_{\mathrm{pre}})_{\mathrm{positive\ seq.}}}{(\underline{I}_{\mathrm{flt}} - \underline{I}_{\mathrm{pre}})_{\mathrm{positive\ seq.}}} \quad (11)$$

The incremental positive sequence impedance enables very reliable direction detection. For a forward fault such the impedance is a local source impedance (as to the value and with the negative sign to account for the fact that the current is flowing from a source to a forward fault location). While for a reverse fault, this impedance equals the line impedance plus the remote source impedance. Certainly, for a series-compensated line, the line impedance must be understood as the line inductive impedance itself plus the capacitive impedance of the series R–C equivalent of the parallel arrangement of a series capacitor and its MOV [1].

Fig. 10 presents performance of the positive-sequence direction element from the substation A under the considered sample a-b fault (Fig. 1 – fault F_2). The computed incremental positive sequence impedances lays in this case basically in the 3rd quadrant (resistance and reactance are negative) and settles at the value equal to the positive sequence impedance of the local source multiplied by (–1). The SCs&MOVs cause large

fluctuations in both resistance and reactance of the incremental positive-sequence impedance. However, basing on the negative sign of the calculated incremental positive-sequence reactance (for all samples except the 1st sample) the forward direction (Fig. 1 – the fault F_2 for the Relay A) is detected reliably and fast.

Fig. 11 presents performance of the positive-sequence direction element from the substation B under the considered sample forward fault. Again, the computed incremental positive-sequence impedances lays in this case basically in the 3rd quadrant and settles at the value equal to the positive sequence impedance of the local source multiplied by (–1). The SCs&MOVs as not contained in the fault-loop basically do not influence the measurement and the calculated quantities are more smooth than in the case of Fig. 10.

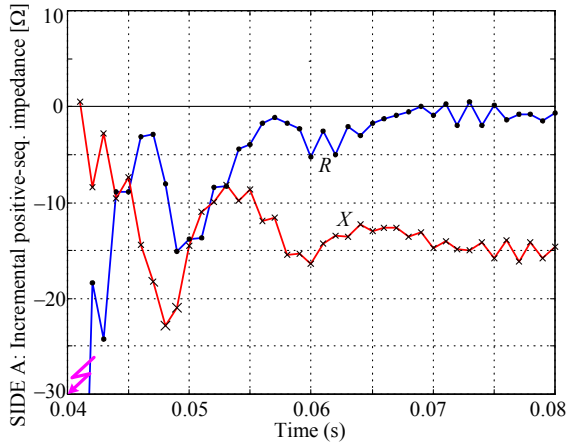

Fig. 10. Fault direction detection by the Relay A from the substation A under the forward fault occurring behind the SCs&MOVs (Fig. 1 - fault F_2).

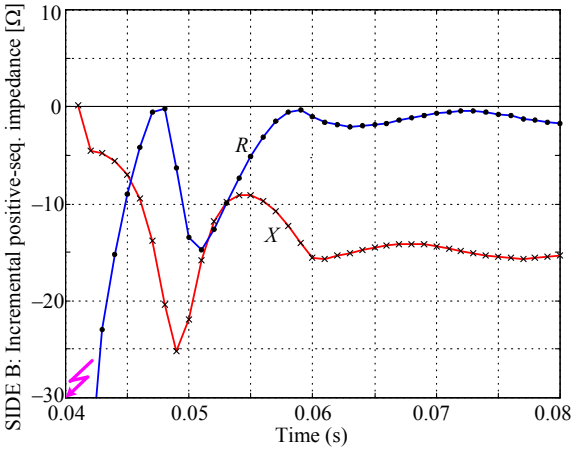

Fig. 11. Fault direction detection by the Relay B from the substation B under the forward fault occurring in front of the SCs&MOVs (Fig. 1 - fault F_2).

Full cycle Fourier filtration was used under determining the sequence components for both the tests (Figs. 10 and 11). The results of the performed tests show that the algorithm based on computing an incremental positive sequence impedance enables reliable and fast fault direction detection in an environment of the studied series compensated network.

VI. Conclusions

Detailed ATP-EMTP model of a single-circuit series compensated line including Metal Oxide Varistors (MOVs), Capacitive Voltage Transformers (CVTs), Current Transformers (CTs) and anti-aliasing analog filters has been developed. Extensive simulation studies have been carried out for a variety of fault conditions with the aim of evaluation of relaying algorithms applied for protection of a series compensated line. Algorithms for impedance measurement and for fault direction discrimination have been studied in details.

For faults behind SCs&MOVs the fundamental frequency based methods introduce considerable delay in addition to the delay caused by their data windows. In turn, the differential equation based methods must be equipped with half-cycle digital pre-filtration otherwise they give poor time responses for faults behind SCs&MOVs. Basing on the presented examples and the performed extensive studies for various faults, finally the method combining the differential equation technique with orthogonal components (subsection C) is finally recommended for fault-loop impedance measurement.

The investigations of this paper have been carried out for fully transposed line. It is expected that the introduced impedance algorithms can be applied for untransposed lines as well, however, this calls for additional investigations.

The phenomena specific to a series compensated line affect the performance of distance relay auxiliary algorithms. Selected results showing performance of the algorithm for fault direction discrimination are presented and discussed.

VII. References

[1] M. M. Saha, J. Izykowski, and E. Rosolowski, *Fault Location on Power Networks*, London, Springer, 2010.

[2] B. Kasztenny, "Distance protection of series compensated lines–problems and solutions," in *Proc. 28th Annual Western Protective Relay Conference*, pp. 1–34, 2001.

[3] M. M. Saha, B. Kasztenny, E. Rosolowski, and J. Izykowski, "First zone algorithm for protection of series compensated lines," *IEEE Trans. Power Delivery*, vol. 16, pp. 200–207, Oct. 2001.

[4] M. M. Saha, J. Izykowski, E. Rosolowski, and B. Kasztenny, "A new accurate fault locating algorithm for series compensated lines," *IEEE Trans. Power Delivery*, vol. 14, pp. 789–797, July 1999.

[5] R. Rubeena, M. R. Dadash Zadeh, and T. P. S. Bains, "An accurate offline phasor estimation for fault location in series-compensated lines," *IEEE Trans. Power Delivery*, vol. 29, pp. 876–883, Apr. 2014.

[6] C. S. Yu, "A reiterative DFT to damp decaying dc and subsynchronous frequency components in fault current," *IEEE Trans. Power Delivery*, vol. 21, pp. 1862–1870, Oct. 2006.

[7] J. C. Gu, K. Y. Shen, S. L. Yu and C. S. Yu, "Removal of DC offset and subsynchronous resonance in current signals for series compensated transmission lines using a novel Fourier filter algorithm," *Elect. Power Syst. Res.*, vol. 76, pp. 327–335, 2006.

[8] P. G. McLaren, G. W. Swift, Z. Zhang, E. Dirks, R. P. Jayasinghle, and I. Fernando, "A new positive sequence directional element for numerical distance relays," in *Proc. of the Stockholm Power Tech Conference, Stockholm*, Sweden, pp. 540-545, 1995.

[9] H. Dommel, *Electromagnetic Transient Program*, BPA, Portland, Oregon, 1986.

[10] H. Hupfauer, P. Schegner and R. Simon, "Distance protection of unsymmetrical lines", *ETEP*, vol. 6, No. 2, pp. 91-96, 1996.

[11] L. B. Jackson, *Digital filters and signal processing*, Kluwer Academic Publishers, 1986.